

Theory of terahertz conductivity in the pseudogap phase of the cuprates: A preformed pair perspective

Dan Wulin and K. Levin*

James Franck Institute and Department of Physics, University of Chicago, Chicago, Illinois 60637, USA
(Received 10 February 2012; revised manuscript received 9 September 2012; published 17 October 2012)

In this paper we deduce transport properties in the presence of a pseudogap associated with precursor superconductivity. Our theoretical analysis is based on the widely adopted self-energy expression reflecting this normal state gap, which has appeared in interpretations of photoemission and in other experiments. Thus, it should be generally applicable. Here we address THz conductivity $\sigma(\omega) = \sigma_1(\omega) + i\sigma_2(\omega)$ measurements in the underdoped high-temperature superconductors and arrive at reasonable agreement between theory and recent experiment for both σ_1 and σ_2 above and below T_c .

DOI: [10.1103/PhysRevB.86.134519](https://doi.org/10.1103/PhysRevB.86.134519)

PACS number(s): 74.72.Kf, 67.85.-d, 74.25.F-

I. INTRODUCTION

One of the biggest challenges in understanding the high-temperature superconductors revolves around the origin of the ubiquitous pseudogap. Because this normal state gap has d-wave-like features compatible with the superconducting order parameter, this suggests that the pseudogap is related to some form of “precursor pairing.” On the other hand, there are many reports^{1,2} suggesting that the pseudogap onset temperature is associated with a broken symmetry and, thus, another order parameter. It is widely believed that because the pseudogap has clear signatures in generalized transport, these measurements^{3,4} may help with the centrally important question of distinguishing the two scenarios. In this paper we analyze recent experimental observations which have suggested that precursor pairing scenarios^{5,6} may be problematic. By default, these observations may imply that the pseudogap must involve another (yet unspecified) order parameter.

Our work is based on a preformed pair scenario,⁷ which has been previously applied to transport⁸⁻¹² within a slightly different, but equivalent, framework. Importantly, this preformed pair scheme is associated with the widely used^{7,13,14} approximate self-energy, which we derived even earlier within our microscopic formalism:^{15,16}

$$\Sigma_{\text{pg},K} = -i\gamma + \frac{\Delta_{\text{pg},\mathbf{k}}^2}{i\omega_n + \xi_{\mathbf{k}} + i\gamma}, \quad (1)$$

where $K = (\mathbf{k}, i\omega_n)$ and $i\omega_n$ is a fermionic Matsubara frequency. Here γ represents a damping, which we will interpret here as related to the interconversion of pairs and fermions. We next show how this self-energy leads very naturally to an expression for the complex conductivity.

II. TRANSPORT THEORY IN THE PRESENCE OF A PREFORMED PAIR-BASED PSEUDOGAP

The complex conductivity can be written in terms of the paramagnetic current-current correlation function $\vec{P}(Q)$ to which one adds the diamagnetic contribution \vec{n}/m :

$$\sigma(\omega) = -\lim_{\mathbf{q} \rightarrow 0} \frac{P_{xx}(\mathbf{q}, \omega) + (n/m)_{xx}}{i\omega}, \quad (2)$$

where the xx subscript denotes the diagonal tensor component along the x direction. We consider in the transverse gauge the linear response of the electromagnetic current $\mathbf{J} = -\vec{K} \mathbf{A}$, to a small vector potential \mathbf{A} . Here $\vec{K}(Q) = \vec{P}(Q) + \vec{n}/m$, where the paramagnetic contribution, given by $\vec{P}(Q)$, is associated with the normal current resulting from fermionic and bosonic excitations. The vector Q is defined as $Q = (\mathbf{q}, i\Omega_m)$, where $i\Omega_m$ is a bosonic Matsubara frequency.

A. Weak dissipation limit

For simplicity, we begin in the weak dissipation limit where the parameter γ in Eq. (1) is small. We define $G_{0,K}^{-1} = (i\omega_n - \xi_{\mathbf{k}})^{-1}$ as the bare Green's function, and show how this standard self-energy expression in the pseudogap state,

$$\Sigma_{\text{pg},K} \approx -\Delta_{\text{pg},\mathbf{k}}^2 G_{0,-K} = \frac{\Delta_{\text{pg},\mathbf{k}}^2}{i\omega_n + \xi_{\mathbf{k}}},$$

leads to consistent expressions for the current-current correlation functions.

We derive an expression for $P(Q)$ by turning first to the diamagnetic current. This can be written as

$$\frac{\overleftarrow{\mathbf{n}}}{m} = 2 \sum_K \frac{\partial^2 \xi_{\mathbf{k}}}{\partial \mathbf{k} \partial \mathbf{k}} G_K = -2 \sum_K \frac{\partial \xi_{\mathbf{k}}}{\partial \mathbf{k}} \frac{\partial G_K}{\partial \mathbf{k}}. \quad (3)$$

The right-hand side of Eq. (3) can be manipulated so that it appears in a form which suggests how to write $\vec{P}(Q)$. First, differentiating both sides of the equality $G_K^{-1} = G_{0,K}^{-1} - \Sigma_{\text{pg},K}$, one has the identity

$$\frac{\partial G_K^{-1}}{\partial \mathbf{k}} = \frac{\partial G_{0,K}^{-1}}{\partial \mathbf{k}} - \frac{\partial \Sigma_{\text{pg},K}}{\partial \mathbf{k}} = -\frac{\partial \xi_{\mathbf{k}}}{\partial \mathbf{k}} - \frac{\partial \Sigma_{\text{pg},K}}{\partial \mathbf{k}}. \quad (4)$$

Using $\partial G_K / \partial \mathbf{k} = -G_K^2 \partial G_K^{-1} / \partial \mathbf{k}$, Eq. (3) becomes

$$\frac{\overleftarrow{\mathbf{n}}}{m} = -2 \sum_K G_K^2 \frac{\partial \xi_{\mathbf{k}}}{\partial \mathbf{k}} \left[\frac{\partial \xi_{\mathbf{k}}}{\partial \mathbf{k}} + \frac{\partial \Sigma_{\text{pg},K}}{\partial \mathbf{k}} \right]. \quad (5)$$

The expression for the self-energy [Eq. (1)] can be used to further simplify Eq. (5). Since $\Sigma_{\text{pg},K} = -\Delta_{\text{pg},\mathbf{k}}^2 G_{0,-K} = \Delta_{\text{pg},\mathbf{k}}^2 (i\omega_n + \xi_{\mathbf{k}})^{-1}$, then

$$\frac{\partial \Sigma_{\text{pg},K}}{\partial \mathbf{k}} = -\Delta_{\text{pg},\mathbf{k}}^2 G_{0,-K}^2 \frac{\partial \xi_{\mathbf{k}}}{\partial \mathbf{k}}, \quad (6)$$

where a term proportional to $\partial\Delta_{\text{pg},\mathbf{k}}/\partial\mathbf{k}$ has been dropped since it gives a negligible contribution to the final result. Therefore Eq. (5) becomes

$$\frac{\overleftrightarrow{n}}{m} = -2\sum_K G_K^2 \frac{\partial\xi_{\mathbf{k}}}{\partial\mathbf{k}} \frac{\partial\xi_{\mathbf{k}}}{\partial\mathbf{k}} (1 - \Delta_{\text{pg},\mathbf{k}}^2 G_{0,-K}^2). \quad (7)$$

Interestingly, the combination GG_0 appears naturally in the manipulations, and this is further exploited in the Appendix to derive a consistent scheme for evaluating the various excitation gaps. In order for the Meissner effect to be present only below T_c we require

$$\overleftrightarrow{P}(0) + \overleftrightarrow{n}/m = 0, \quad T \geq T_c, \quad (8)$$

which results in

$$\overleftrightarrow{P}(0) = 2\sum_K \frac{\partial\xi_{\mathbf{k}}}{\partial\mathbf{k}} \frac{\partial\xi_{\mathbf{k}}}{\partial\mathbf{k}} [G_K G_K (1 - \Delta_{\text{pg},\mathbf{k}}^2 G_{0,-K}^2)]. \quad (9)$$

A natural extension of Eq. (9) to general Q is

$$\overleftrightarrow{P}(Q) = 2\sum_K \frac{\partial\xi_{\mathbf{k}+\mathbf{q}/2}}{\partial\mathbf{k}} \frac{\partial\xi_{\mathbf{k}+\mathbf{q}/2}}{\partial\mathbf{k}} [G_K G_{K+Q} - \Delta_{\text{pg},\mathbf{k}} \Delta_{\text{pg},\mathbf{k}+\mathbf{q}} G_{0,-K-Q} G_{0,-K} G_{K+Q} G_K]. \quad (10)$$

This ansatz will be checked by appealing to the transverse f-sum rule. First, we rewrite Eq. (10) as

$$\begin{aligned} P_{xx}(\mathbf{q},\omega) &= \sum_{\mathbf{k}} \frac{\partial\xi_{\mathbf{k}}}{\partial k_x} \frac{\partial\xi_{\mathbf{k}}}{\partial k_x} \left[\frac{E_{\mathbf{k}}^+ + E_{\mathbf{k}}^-}{E_{\mathbf{k}}^+ E_{\mathbf{k}}^-} \frac{E_{\mathbf{k}}^+ E_{\mathbf{k}}^- - \xi_{\mathbf{k}}^+ \xi_{\mathbf{k}}^- - \delta\Delta_{\mathbf{k},\mathbf{q}}^2}{\omega^2 - (E_{\mathbf{k}}^+ + E_{\mathbf{k}}^-)^2} \right. \\ &\quad \times (1 - f(E_{\mathbf{k}}^+) - f(E_{\mathbf{k}}^-)) - \frac{E_{\mathbf{k}}^+ - E_{\mathbf{k}}^-}{E_{\mathbf{k}}^+ E_{\mathbf{k}}^-} \\ &\quad \left. \times \frac{E_{\mathbf{k}}^+ E_{\mathbf{k}}^- + \xi_{\mathbf{k}}^+ \xi_{\mathbf{k}}^- + \delta\Delta_{\mathbf{k},\mathbf{q}}^2}{\omega^2 - (E_{\mathbf{k}}^+ - E_{\mathbf{k}}^-)^2} (f(E_{\mathbf{k}}^+) - f(E_{\mathbf{k}}^-)) \right], \quad (11) \end{aligned}$$

where a \pm superscript indicates that the given function is evaluated at $\mathbf{k} \pm \mathbf{q}/2$. We define

$$\delta\Delta_{\mathbf{k},\mathbf{q}}^2 = -\Delta_{\text{pg},\mathbf{k}}^+ \Delta_{\text{pg},\mathbf{k}}^-, \quad T \geq T_c. \quad (12)$$

Once the temperature passes below T_c , we need to include the self-energy of the condensed pairs as well:

$$\Sigma_K = \Sigma_{\text{sc},K} + \Sigma_{\text{pg},K} = -[\Delta_{\text{pg},\mathbf{k}}^2 + \Delta_{\text{sc},\mathbf{k}}^2] G_{0,-K}, \quad (13)$$

where Σ_K now consists of a condensed and noncondensed pair contributions. This results in an expression for the diamagnetic

contribution, just as in Eq. (9), which can be rewritten in the form

$$\frac{\overleftrightarrow{n}}{m} = 2\sum_{\mathbf{k}} \frac{\partial\xi_{\mathbf{k}}}{\partial\mathbf{k}} \frac{\partial\xi_{\mathbf{k}}}{\partial\mathbf{k}} \left[\frac{\Delta_{\mathbf{k}}^2}{E_{\mathbf{k}}^2} \frac{1 - 2f(E_{\mathbf{k}})}{2E_{\mathbf{k}}} - \frac{\xi_{\mathbf{k}}^2}{E_{\mathbf{k}}^2} \frac{\partial f(E_{\mathbf{k}})}{\partial E_{\mathbf{k}}} \right], \quad (14)$$

where $\Delta_{\mathbf{k}}^2 = \Delta_{\text{pg},\mathbf{k}}^2 + \Delta_{\text{sc},\mathbf{k}}^2$. To determine how $\Delta_{\text{sc},\mathbf{k}}^2$ enters into the paramagnetic current $P(Q)$, we observe that, in the BCS limit,

$$\delta\Delta_{\mathbf{k},\mathbf{q}}^2 = \Delta_{\text{sc},\mathbf{k}}^+ \Delta_{\text{sc},\mathbf{k}}^-, \quad \text{BCS limit.}$$

An essential point is that the superconducting gap $\Delta_{\text{sc},\mathbf{k}}$ appears with the opposite sign from the pseudogap contribution in Eq. (12). In the case of general temperatures, $0 \leq T \leq T_c$, we combine the two limits to yield the appropriate form for the quantity

$$\delta\Delta_{\mathbf{k},\mathbf{q}}^2 = \Delta_{\text{sc},\mathbf{k}}^+ \Delta_{\text{sc},\mathbf{k}}^- - \Delta_{\text{pg},\mathbf{k}}^+ \Delta_{\text{pg},\mathbf{k}}^-, \quad (15)$$

which enters into Eq. (11). Importantly, Eqs. (11) and (15) represent the full electromagnetic response above and below T_c , albeit in the weak dissipation limit. The superfluid density follows from the definition

$$\overleftrightarrow{P}(0) + \overleftrightarrow{n}/m = \overleftrightarrow{n}_s/m. \quad (16)$$

Combining Eq. (11), (15), and (14) implies that the superfluid density is given by

$$\frac{n_s}{m} = 2\sum_{\mathbf{k}} \frac{\partial\xi_{\mathbf{k}}}{\partial k_x} \frac{\partial\xi_{\mathbf{k}}}{\partial k_x} \frac{\Delta_{\text{sc},\mathbf{k}}^2}{E_{\mathbf{k}}^2} \left[\frac{1 - 2f(E_{\mathbf{k}})}{2E_{\mathbf{k}}} + \frac{\partial f(E_{\mathbf{k}})}{\partial E_{\mathbf{k}}} \right]. \quad (17)$$

Thus the normal fluid density, which will be used as input into the f-sum rule that constrains $\sigma_1(\omega)$, is

$$\begin{aligned} n_n/m &= n/m - n_s/m \\ &= 2\sum_{\mathbf{k}} \frac{\partial\xi_{\mathbf{k}}}{\partial k_x} \frac{\partial\xi_{\mathbf{k}}}{\partial k_x} \left[\frac{\Delta_{\text{pg},\mathbf{k}}^2}{E_{\mathbf{k}}^2} \frac{1 - 2f(E_{\mathbf{k}})}{2E_{\mathbf{k}}} \right. \\ &\quad \left. - \frac{E_{\mathbf{p}}^2 - \Delta_{\text{pg},\mathbf{k}}^2}{E_{\mathbf{k}}^2} \frac{\partial f(E_{\mathbf{k}})}{\partial E_{\mathbf{k}}} \right] \end{aligned}$$

The transverse f-sum rule is given by

$$\lim_{q \rightarrow 0} \int_{-\infty}^{+\infty} \frac{d\omega}{\pi} \left(-\frac{\text{Im}P_{xx}(\mathbf{q}, i\Omega_m \rightarrow \omega + i0^+)}{\omega} \right) = \frac{n_n}{m}. \quad (18)$$

This sum rule can be proven to hold analytically by directly using Eq. (11), along with the normal fluid density. From Eq. (11), we have

$$\begin{aligned} &\lim_{q \rightarrow 0} \int_{-\infty}^{+\infty} \frac{d\omega}{\pi} \left(-\frac{\text{Im}P_{xx}(\mathbf{q}, i\Omega_m \rightarrow \omega + i0^+)}{\omega} \right) \\ &= \sum_{\mathbf{p}} \frac{1}{2} \frac{\partial\xi_{\mathbf{k}}}{\partial k_x} \frac{\partial\xi_{\mathbf{k}}}{\partial k_x} \left[\frac{E_{\mathbf{k}}^2 - E_{\mathbf{k}}^2 + 2\Delta_{\text{pg},\mathbf{k}}^2}{E_{\mathbf{k}}^2} \left(\frac{1}{2E_{\mathbf{k}}} - \frac{1}{-2E_{\mathbf{k}}} \right) (1 - 2f(E_{\mathbf{k}})) - 2 \frac{E_{\mathbf{k}}^2 + E_{\mathbf{k}}^2 - 2\Delta_{\text{pg},\mathbf{k}}^2}{E_{\mathbf{k}}^2} \lim_{q \rightarrow 0} \frac{f(E_{\mathbf{k}}^+) - f(E_{\mathbf{k}}^-)}{E_{\mathbf{k}}^+ - E_{\mathbf{k}}^-} \right] \\ &= 2\sum_{\mathbf{k}} \frac{\partial\xi_{\mathbf{k}}}{\partial k_x} \frac{\partial\xi_{\mathbf{k}}}{\partial k_x} \left[\frac{\Delta_{\text{pg},\mathbf{k}}^2}{E_{\mathbf{k}}^2} \frac{1 - 2f(E_{\mathbf{k}})}{2E_{\mathbf{k}}} - \frac{E_{\mathbf{p}}^2 - \Delta_{\text{pg},\mathbf{k}}^2}{E_{\mathbf{k}}^2} \frac{\partial f(E_{\mathbf{k}})}{\partial E_{\mathbf{k}}} \right] = \frac{n_n}{m}. \quad (19) \end{aligned}$$

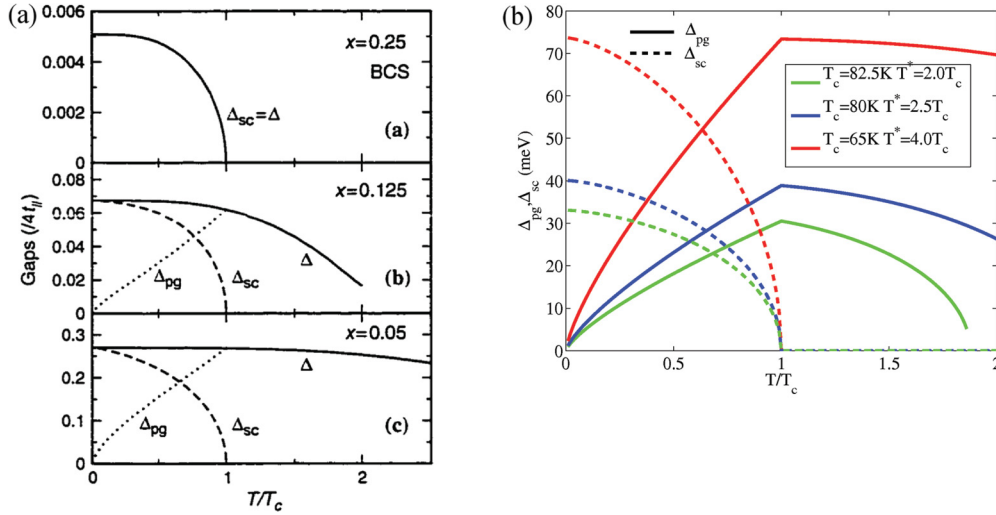


FIG. 1. (Color online) (a) The superconducting gap Δ_{sc} and pseudogap Δ_{pg} at the antinode for three different dopings and in units of the in-plane hopping integral $t_{||}$, obtained self-consistently within the microscopic model discussed here for a nearest neighbor tight-binding dispersion, as a function of temperature. Temperature is measured in units of the transition temperature T_c . Solid lines show Δ , dotted lines Δ_{pg} , and dashed lines Δ_{sc} (from Ref. 17). (b) The gaps used for the present calculations. Superconducting gap Δ_{sc} and pseudogap Δ_{pg} at the antinode in meV for three different dopings as functions of temperature. Temperature is measured in units of the transition temperature T_c . The solid lines show Δ_{pg} , and dashed lines denote Δ_{sc} . Here $\Delta^2 = \Delta_{sc}^2 + \Delta_{pg}^2$ represents the square of the excitation gap. Details of these parameters are included in Ref. 18.

Importantly one can see by direct Kramers Kronig analysis that Eq. (8), which reflects the absence of a normal state Meissner effect, is intimately connected to the sum rule above T_c .

The confirmation of the sum rule then serves to validate Eq. (11), where importantly Eq. (15) must be used. This theory was discussed in the context of the more microscopic model derived in the Appendix and Ref. 19. We stress that in the usual BCS-like, purely fermionic Hamiltonian (which we consider here) only fermions possess a hopping kinetic energy and thereby directly contribute to transport, as indicated by the right-hand side of the sum rule. The contribution to transport from pair-correlated fermions enters indirectly by liberating these fermions through a break-up of the pairs.

We now see that the general form of the superconducting electromagnetic response consists of three distinct contributions: (1) superfluid acceleration, (2) quasiparticle scattering, and (3) pair breaking and pair forming. These all appear in conventional BCS superconductors, but at $T = 0$ this last effect is present only when there is disorder. However, in the presence of stronger than BCS attraction and at $T \neq 0$, noncondensed pairs can be decomposed to add to the higher frequency conductivity.

B. Strong dissipation limit

We now use the full expression for the self-energy to obtain compatible expressions for transport coefficients in the strong dissipation limit.⁹ The full Green's function is given by

$$G_K = \left(i\omega_n - \xi_{\mathbf{k}} + i\gamma - \frac{\Delta_{pg,\mathbf{k}}^2}{i\omega_n + \xi_{\mathbf{k}} + i\gamma} - \frac{\Delta_{sc,\mathbf{k}}^2}{i\omega_n + \xi_{\mathbf{k}}} \right)^{-1}. \quad (20)$$

Below T_c we introduce terms of the form $F_{sc,K} F_{sc,K+Q}$, which represent the usual Gor'kov functions to represent the

condensate. More specifically, $F_{sc,K}$ can be represented as a product of one dressed and one bare Green's function (GG_0):

$$F_{sc,K} \equiv -\frac{\Delta_{sc,\mathbf{k}}}{i\omega_n + \xi_{\mathbf{k}}} \frac{1}{i\omega_n - \xi_{\mathbf{k}} - \frac{\Delta_{\mathbf{k}}^2}{i\omega_n + \xi_{\mathbf{k}}}}. \quad (21)$$

This natural extension of our small dissipation result leads to

$$\vec{P}(Q) \approx 2 \sum_K \frac{\partial \xi_{\mathbf{k}+Q/2}}{\partial \mathbf{k}} \frac{\partial \xi_{\mathbf{k}+Q/2}}{\partial \mathbf{k}} [G_K G_{K+Q} + F_{sc,K} F_{sc,K+Q} - F_{pg,K} F_{pg,K+Q}], \quad (22)$$

where $F_{pg,K} \equiv -\Delta_{pg,\mathbf{k}}(i\omega_n + \xi_{\mathbf{k}} + i\gamma)^{-1} G_K$. Here the $F_{pg,K}$ terms represent the noncondensed pair contribution to transport, which appeared in our small dissipation derivation as well. They are not to be associated with broken symmetry. This is, in part, reflected in the incorporation of the finite lifetime γ^{-1} in the expression for $F_{pg,K}$. Rather they represent correlations among pairs of fermions. This is in contrast to the $F_{sc,K}$ contributions, which are present only for $T \leq T_c$ and reflect a nonzero order parameter $\Delta_{sc,\mathbf{k}}$. Note that the difference in the relative signs of $\Delta_{pg,\mathbf{k}}^2$ and $\Delta_{sc,\mathbf{k}}^2$ that appears in Eq. (23) is a direct consequence of the same physics discussed in our weak dissipation calculations. That the condensed and noncondensed pairs enter in a different fashion is a crucial finding and one that is essential in order that the noncondensed pairs do not contribute to a Meissner effect.

III. CALCULATION OF THE PAIRING GAPS

Throughout this paper we have implicitly presumed that the gap components $\Delta_{pg}(T)$ and $\Delta_{sc}(T)$ are known, where the gaps are assumed to be d-wave and $\Delta_{pg}(T)$ and $\Delta_{sc}(T)$ are the gap magnitudes at the antinodes. We now discuss the

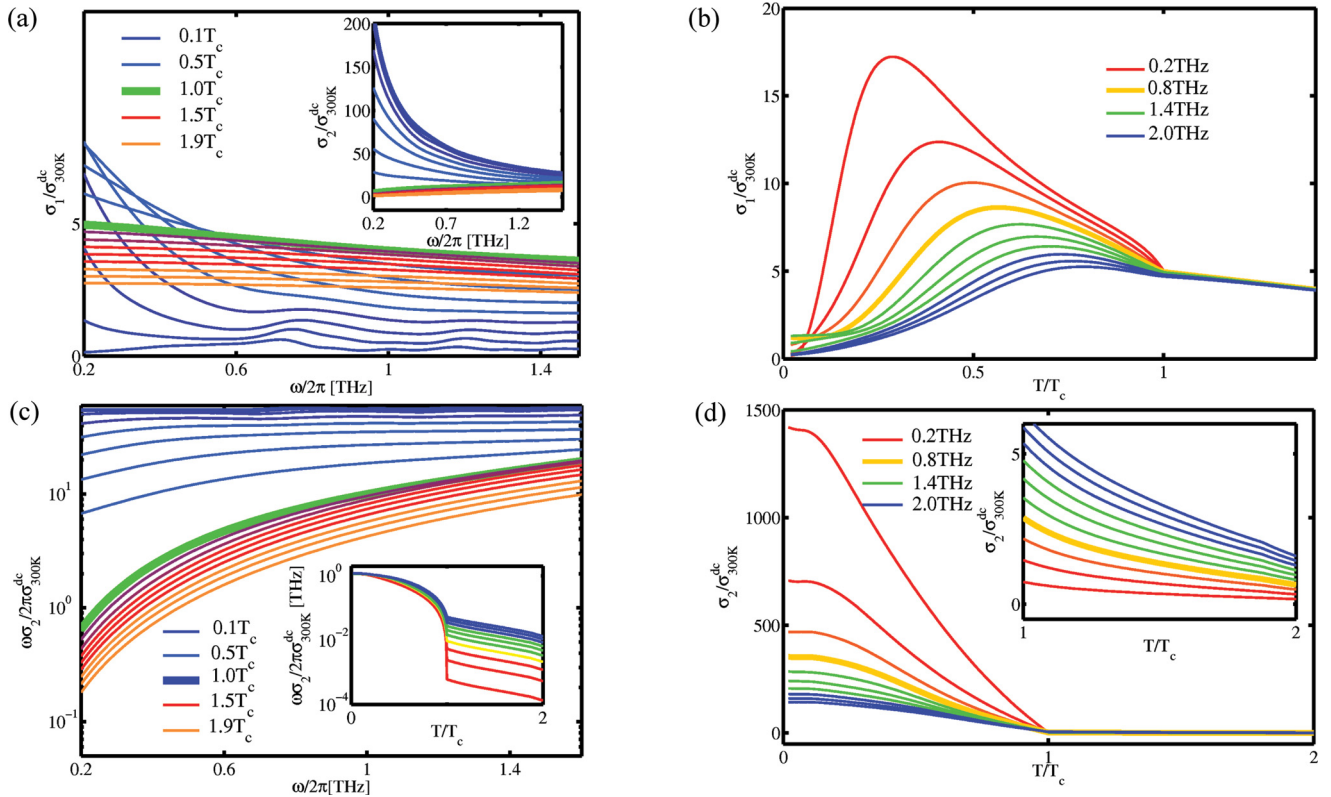


FIG. 2. (Color online) (a) The real conductivity σ_1 as a function of frequency normalized by the dc conductivity at $T = 300$ K, $\sigma_{300\text{K}}^{\text{dc}}$. Inset: The imaginary conductivity σ_2 as a function of frequency. (b) The real conductivity σ_1 as a function of temperature. (c) The quantity $\omega\sigma_2$ as a function of frequency. Inset: $\omega\sigma_2$ as a function of temperature. (d) The imaginary conductivity σ_2 as a function of temperature. Inset: σ_2 as a function of temperature near T_c .

way in which these are calculated, referring the reader to the Appendix for more details.

We consider a preformed pair scenario, which is based on BCS-Bose Einstein condensation (BCS-BEC) theory. Given the small pair size and the anomalously high transition temperatures of the cuprates, one might associate these findings with a stronger than BCS attractive interaction. Importantly, the BCS ground state wave function

$$|\Psi_0\rangle = \prod_{\mathbf{k}} (u_{\mathbf{k}} + v_{\mathbf{k}} c_{\mathbf{k},\uparrow}^\dagger c_{-\mathbf{k},\downarrow}^\dagger) |0\rangle \quad (23)$$

is well known to contain both the BCS and BEC limits. We present in the Appendix a treatment of finite temperature effects which is based on a t-matrix implementation of BCS-BEC theory. Ours represents a straightforward extension of standard BCS and Gor'kov theory. Given that we start with the same wave function, it is not surprising that our pairing scenario is a mean-field scheme just as in strict BCS theory. Beyond this BCS endpoint there are two types of excitations, fermionic quasiparticles and pair excitations. The fermions have the usual dispersion relation $E_{\mathbf{k}}$, where $E_{\mathbf{k}} \equiv \sqrt{\xi_{\mathbf{k}} + \Delta_{\mathbf{k}}^2}$ and where the excitation gap consists of two contributions from noncondensed (pg) and condensed (sc) pairs: via $\Delta_{\mathbf{k}}^2 \equiv \Delta_{\text{pg},\mathbf{k}}^2 + \Delta_{\text{sc},\mathbf{k}}^2$. We stress that the preformed pairs represent pair correlations of fermions which have nothing to do with broken symmetry. Note that the full gap $\Delta_{\mathbf{k}}$ remains relatively T-independent, even below T_c because of the conversion

of noncondensed ($\Delta_{\text{pg},\mathbf{k}}$) to condensed ($\Delta_{\text{sc},\mathbf{k}}$) pairs as the temperature is lowered.

Written in terms of fermion creation and annihilation operators (c^\dagger and c , respectively), these pair correlations correspond to $[\langle cc^\dagger cc^\dagger \rangle - \langle c^\dagger c^\dagger \rangle \langle cc \rangle]$ and are ignored in BCS theory (where the attraction is very weak). In a closely related fashion, the (square of the) contribution to the total pairing gap $[\Delta(T)]$ associated with noncondensed pairs (pg) can be written⁷ as $\Delta_{\text{pg}}^2(T) = [\Delta^2(T) - \Delta_{\text{sc}}^2(T)]$, where sc corresponds to condensed pairs and pg corresponds to the preformed (pseudogap) pairs.

The results of a full numerical solution¹⁷ for these gap parameters [associated with Eqs. (A6), (A9), and (A10)] for a nearest-neighbor tight-binding dispersion is shown in Fig. 1(a), where the gaps Δ , Δ_{sc} , and Δ_{pg} are plotted as functions of temperature and for different dopings, as represented by different interaction coupling constants. For the calculations performed in this paper, the specific parameters that were used are illustrated in Fig. 1(b). These particular parameters were chosen for consistency with the cuprate phase diagram, so that, for example, the attractive interaction was chosen to fit T^* . This procedure is described in more detail in Ref. 18.

IV. DETAILED NUMERICAL STUDIES

We now turn to more detailed comparisons between the theory of the conductivity and experiment. Figure 2 displays our more quantitative results for σ_1 and σ_2 both as functions of

ω and T . Our numerical results, based on Eq. (2), are presented in a layout designed to mirror Fig. 1 from Ref. 5 where the general trends are similar. One sees from Fig. 2(a) and its inset that well above T_c , the real part of the conductivity is almost frequency independent. The imaginary part is small in this regime. At the lowest temperatures σ_1 contains much reduced spectral weight while the frequency dependence of $\sigma_2 \propto \omega^{-1}$; both of these reflect the characteristic behavior of a superfluid. The behavior below T_c is not superficially different from that of strict BCS theory. However, it should be noted that the pairing gap $\Delta(T)$ (at the antinodes) is almost T independent. BCS theory (which considers only fermionic excitations) would, thus, predict no significant T dependences in σ_1 and σ_2 .

Here, as in the experimental studies,⁵ we focus primarily on the temperature dependent plots in Figs. 2(b), 2(d), and the inset to 2(c). One sees that σ_1 shows a slow decrease as the temperature is raised above T_c . Somewhat below T_c , σ_1 exhibits a peak that occurs at progressively lower temperatures as the probe frequency is decreased. At roughly T_c , we find that σ_2 shows a sharp upturn at low ω . The region of finite σ_2 above the transition can be seen from the inset in Fig. 2(d). The inset shows an expanded view of $\sigma_2(T)$ near T_c . In agreement with experiment, the nesting of the σ_2 versus T curves switches orders above T_c .

These effects are made clearer by plotting the “phase stiffness,” which is proportional to the quantity $\omega\sigma_2$ and is shown in Fig. 2(c). Deep in the superconducting state there is no ω dependence to $\omega\sigma_2(\omega)$, while at higher T this dependence becomes apparent. In the inset to Fig. 2(c), the temperature dependence of $\omega\sigma_2(T)$ is displayed. We see that above T_c , $\omega\sigma_2$ is never strictly constant, as would be expected from fluctuation contributions.

In general, these curves capture the qualitative features observed in recent experiments.⁵

V. CONCLUSIONS

In this paper we have shown how the standard self-energy expression ($\Sigma_{\text{pg},\kappa}$) which appears in Eq. (1) and which is widely adopted in the literature^{7,13,14} can be used to derive the frequency dependent conductivity $\sigma(\omega)$. Importantly, the results can be seen to be analytically compatible with the transverse f-sum rule, and semiquantitatively compatible with the data. In the normal state this constraint is equivalent to the requirement that there is no Meissner effect. This theory is readily extended below T_c by including a second component to the excitation gap associated with condensed pairs which is of the usual BCS (undamped) form. We have additionally shown that the recent experiments by Bilbro *et al.*⁵ can be successfully addressed in this framework, which can be microscopically associated with BCS-BEC crossover theory. Importantly, this particular variant of a preformed pair approach has been unambiguously realized in (atomic physics) experiments where a pseudogap is claimed to be observed.²⁰

We can summarize the effects of a pseudogap in the normal state, which differentiates the present theory from that of its BCS counterpart. In the low-frequency regime, with a pseudogap present, there are fewer fermions available to contribute to transport since their number is reduced because

they are tied up into pairs. However, once the frequency is sufficiently high to break the pairs into individual fermions, the conductivity rises above that of the Drude model. One can see that the effect of the pseudogap is to transfer the spectral weight from low frequencies to higher energies, $\omega \approx 2\Delta$ (where Δ is the pairing gap). In this way one finds an extra “midinfrared” contribution to the conductivity,²¹ which is as observed²² experimentally and is strongly tied to the presence of a pseudogap. This contribution is not, however, visible in the low ω THz experiments that are considered in this paper.

The behavior of $\sigma_2(\omega)$ is rather similarly constrained. On general principles, σ_2 must vanish at strictly zero frequency as long as the system is normal. Here one can see that the low-frequency behavior is also suppressed by the presence of a pseudogap because of the gap-induced decrease in the number of carriers. At higher $\omega \approx 2\Delta$, the second peak in $\sigma_1(\omega)$ leads, via a Kramers-Kronig transform to a slight depression in $\sigma_2(\omega)$ in this frequency range. As a result, $\sigma_2(\omega)$ is significantly reduced relative to the Drude result.

We now turn to the question of to what extent does the conductivity below the transition temperature differ from that in strict BCS theory. Here it is important to stress the complexity of the superfluid phase in the presence of a pseudogap. Angle resolved photoemission experiments²³ indicate that the (antinodal) spectral gap is not sensitive to T_c . In strict BCS theory with a constant pairing gap, the superfluid density should not vanish at T_c . Rather, it would vanish when the excitation gap disappeared, say, at T^* . Moreover, since $\sigma_2 \propto n_s/\omega$ it would then seem to be difficult to understand the behavior of the THz conductivity, which reflects T_c and not T^* .

There has to be, therefore, a substantial effect of the pseudogap which persists below T_c , thus differentiating these systems from conventional BCS superconductors. In the present theory this difference is incorporated by including a nonzero Δ_{pg} , to be associated with noncondensed pairs which are present above T_c and do not immediately disappear once the transition line is crossed. Rather, these noncondensed pairs gradually convert to the condensate as $T \rightarrow 0$. As a consequence, in the present approach we find that the spectral gap exhibits the T insensitivity at the antinodes¹⁸ while n_s ⁸ vanishes at T_c and appears clearly in transport.

Finally, we raise the important issue of concomitant order in the above T_c pseudogap phase. Interestingly, we have found such order to exist in high magnetic fields, in the form of bosonic charge density wave-like states or precursor vortex configurations. Future work will be required to see if this is a more general phenomenon. Nevertheless, it should be clear that the THz conductivity and even the two-gap physics observed in ARPES²³ are not incompatible with a preformed pair scenario for the cuprates. They, thus, do not necessarily require the presence of another order parameter.

ACKNOWLEDGMENTS

This work is supported by NSF-MRSEC Grant 0820054. We thank Hao Guo and Chih-Chun Chien, along with Peter Scherpelz and A. Varlamov for useful conversations, and L. Bilbro and N. P. Armitage for sharing unpublished data.

APPENDIX: SUMMARY OF T-MATRIX THEORY

In this section we summarize previous work^{8,19,24} which established a microscopic description of the pseudogap based on BCS-BEC theory. It led as well to the expression for the response function used here. Alternative formulations of preformed pairs of a different nature from our work are discussed in Ref. 25. In the present paper a stronger than BCS attraction leads to boson-like excitations or metastable, long-lived pairs with nonzero net momentum. These pairs give rise to a gap for fermionic excitations. At the microscopic level these pairs are associated with a t-matrix, which is coupled to the fermionic Green's function, which is, in turn, dependent on the t-matrix.

It is useful to begin by reformulating strict BCS theory as a BEC phenomenon which motivates our extension to treat a stronger than BCS attraction. Important here is that BCS theory can be viewed as incorporating *virtual* noncondensed pairs. Here we consider the general case applicable to both s- and d-wave pairing by defining the form factor $\varphi_{\mathbf{k}} = [\cos(k_x) - \cos(k_y)]$ for the latter and taking it to be unity for the former. These virtual $Q \neq 0$ pairs are associated with an effective propagator or t-matrix, which is taken to be of the form

$$t(Q) \equiv \frac{U}{1 + U \sum_{\mathbf{K}} G_{\mathbf{K}} G_{0,-\mathbf{K}+Q} \varphi_{\mathbf{k}-\mathbf{q}/2}^2} \quad (\text{A1})$$

in order to yield the standard BCS equations. This t-matrix incorporates a summation of ladder diagrams in the particle-particle channel and importantly depends on both G and G_0 , which represent dressed and noninteracting Green's functions, respectively. That one has this mixture of the two Green's functions can be traced back to the gap equation of Gor'kov theory. In order to describe pairing in the $d_{x^2-y^2}$ -wave channel, we write the attractive fermion-fermion interaction in the form $U_{\mathbf{k},\mathbf{k}'} = U \varphi_{\mathbf{k}} \varphi_{\mathbf{k}'}$, where U is the strength of the pairing interaction. As in bosonic theories, noncondensed pair excitations of the condensate are necessarily gapless below T_c . This means that $t(Q \rightarrow 0) \rightarrow \infty$ and is equivalent to the vanishing of the effective pair chemical potential μ_{pair} for $T \leq T_c$. This leads to a central constraint on the T -matrix $t^{-1}(Q \rightarrow 0) = 0 \rightarrow \mu_{\text{pair}} = 0, T \leq T_c$. In order to identify the above condition with the BCS gap equation, we need to incorporate the appropriate form for $G_{\mathbf{K}}$. In BCS theory the fermionic self-energy that appears in the fully dressed Green's function $G_{\mathbf{K}}$ is

$$\begin{aligned} \Sigma_{\text{sc},\mathbf{K}} &= \sum_Q t_{\text{sc}}(Q) G_{0,-\mathbf{K}+Q} \varphi_{\mathbf{k}-\mathbf{q}/2}^2 \\ &= - \sum_Q \Delta_{\text{sc},\mathbf{k}}^2 \delta(Q) G_{0,-\mathbf{K}+Q} \\ &= -\Delta_{\text{sc},\mathbf{k}}^2 G_{0,-\mathbf{K}}, \end{aligned} \quad (\text{A2})$$

where $\Delta_{\text{sc},\mathbf{k}}(T) \equiv \Delta_{\text{sc}}(T) \varphi_{\mathbf{k}}$ is the superconducting order parameter. The full Green's function is then $G_{\mathbf{K}}^{-1} = G_{0,\mathbf{K}}^{-1} - \Sigma_{\text{sc},\mathbf{K}}$, which, when inserted in Eq. (A1), yields the BCS gap equation below T_c : $1 = -U \sum_{\mathbf{k}} \frac{1-2f(E_{\mathbf{k}}^{\text{sc}})}{2E_{\mathbf{k}}^{\text{sc}}} \varphi_{\mathbf{k}}^2$ with $E_{\mathbf{k}}^{\text{sc}} \equiv \sqrt{\xi_{\mathbf{k}}^2 + \Delta_{\text{sc},\mathbf{k}}^2}$. We have thus used Eq. (A1) to derive the standard BCS gap equation within a t-matrix language. Importantly, this demonstrates that we can interpret this gap equation as a BEC

condition. That is, it is an extended version of the Thouless criterion of the strict BCS theory that applies for all $T \leq T_c$.

In order to extend the t-matrix theory to include a stronger than BCS attraction we presume that the $Q \neq 0$ pairs are no longer virtual. The t-matrix in general possesses two contributions: the $\mathbf{q} = 0$ contribution that gives rise to the condensed or superconducting pairs and the $\mathbf{q} \neq 0$ contribution of Eq. (A1) that describes the correlations associated with the noncondensed pairs. As a result, the fermionic self-energy also possesses two contributions that are given by

$$\begin{aligned} \Sigma_{\mathbf{K}} &= \sum_Q t(Q) G_{0,-\mathbf{K}+Q} \varphi_{\mathbf{k}-\mathbf{q}/2}^2 \\ &= \sum_Q [t_{\text{sc}}(Q) + t_{\text{pg}}(Q)] G_{0,-\mathbf{K}+Q} \varphi_{\mathbf{k}-\mathbf{q}/2}^2 = \Sigma_{\text{sc},\mathbf{K}} + \Sigma_{\text{pg},\mathbf{K}}. \end{aligned} \quad (\text{A3})$$

The resulting full Green's function is $G_{\mathbf{K}}^{-1} = G_{0,\mathbf{K}}^{-1} - \Sigma_{\text{sc},\mathbf{K}} - \Sigma_{\text{pg},\mathbf{K}}$. While, as before, $\Sigma_{\text{sc},\mathbf{K}} = -\Delta_{\text{sc},\mathbf{k}}^2 G_{0,-\mathbf{K}}$, we find numerically^{15,16} that $\Sigma_{\text{pg},\mathbf{K}}$ is in general of the form

$$\Sigma_{\text{pg},\mathbf{K}} \approx \frac{\Delta_{\text{pg},\mathbf{k}}^2}{\omega + \xi_{\mathbf{k}} + i\gamma} \quad (\text{A4})$$

with $\Delta_{\text{pg},\mathbf{k}} = \Delta_{\text{pg}} \varphi_{\mathbf{k}}$. That is, the self-energy associated with the noncondensed pairs possesses the same structure as its BCS counterparts, albeit with a finite lifetime, γ^{-1} .

We can understand these results more physically as arising from the fact that $t_{\text{pg}}(Q)$ is strongly peaked around $Q = 0$ below T_c where the pair chemical potential is zero and for a range of temperatures above T_c as well where this chemical potential is small. Thus the bulk of the contribution to $\Sigma_{\text{pg},\mathbf{K}}$ in the ordered state comes from small Q :

$$\Sigma_{\text{pg},\mathbf{K}} \approx - \sum_Q t_{\text{pg}}(Q) G_{0,-\mathbf{K}}. \quad (\text{A5})$$

If we define

$$\Delta_{\text{pg},\mathbf{k}}^2 \equiv - \sum_Q t_{\text{pg}}(Q) \varphi_{\mathbf{k}}^2, \quad (\text{A6})$$

we may write

$$\Sigma_{\mathbf{K}} \approx -(\Delta_{\text{sc},\mathbf{k}}^2 + \Delta_{\text{pg},\mathbf{k}}^2) G_{0,-\mathbf{K}} \equiv -\Delta_{\mathbf{k}}^2 G_{0,-\mathbf{K}}. \quad (\text{A7})$$

Equation (A5) leads to an effective pairing gap $\Delta(T)$ whose square is associated with the sum of the squares of the condensed and noncondensed contributions

$$\Delta_{\mathbf{k}}^2(T) = \Delta_{\text{sc},\mathbf{k}}^2(T) + \Delta_{\text{pg},\mathbf{k}}^2(T). \quad (\text{A8})$$

Note that the full gap $\Delta_{\mathbf{k}}$ remains relatively T -independent, even below T_c because of the conversion of noncondensed ($\Delta_{\text{pg},\mathbf{k}}$) to condensed ($\Delta_{\text{sc},\mathbf{k}}$) pairs as the temperature is lowered. The gap equation for this pairing gap, $\Delta_{\mathbf{k}}(T) = \Delta(T) \varphi_{\mathbf{k}}$, is again obtained from the condition $t_{\text{pg}}^{-1}(Q = 0) = 0$, and given by

$$1 = -U \sum_{\mathbf{k}} \frac{1-2f(E_{\mathbf{k}})}{2E_{\mathbf{k}}} \varphi_{\mathbf{k}}^2, \quad (\text{A9})$$

where $E_{\mathbf{k}} \equiv \sqrt{\xi_{\mathbf{k}}^2 + \Delta^2(T) \varphi_{\mathbf{k}}^2}$, and f is the Fermi distribution function. Note that one needs to self-consistently determine the fermionic chemical potential, μ , by conserving the number of

particles, $n = 2 \sum_K G_K$, which leads to

$$n = 2 \sum_K G_K = \sum_{\mathbf{k}} \left[1 - \frac{\xi_{\mathbf{k}}}{E_{\mathbf{k}}} + 2 \frac{\xi_{\mathbf{k}}}{E_{\mathbf{k}}} f(E_{\mathbf{k}}) \right]. \quad (\text{A10})$$

Equations (A6), (A9), and (A10) present a closed set of equations for the chemical potential μ , the pairing gap $\Delta_{\mathbf{k}}(T) = \Delta(T)\varphi_{\mathbf{k}}$, the pseudogap $\Delta_{\text{pg},\mathbf{k}}(T) \equiv \Delta_{\text{pg}}(T)\varphi_{\mathbf{k}}$, and

the superconducting order parameter $\Delta_{\text{sc},\mathbf{k}}(T) = \Delta_{\text{sc}}\varphi_{\mathbf{k}}$ with $\Delta_{\text{sc}}(T) = \sqrt{\Delta^2(T) - \Delta_{\text{pg}}^2(T)}$. We find that $\Delta_{\text{pg}}(T)$ essentially vanishes at $T = 0$ where $\Delta = \Delta_{\text{sc}}$. In this way, the “two gap” physics disappears in the ground state. Importantly, numerical studies²⁶ show that for d-wave pairing, there is no superfluid phase in the bosonic regime where μ is negative; the pseudogap is thus associated with the fermionic regime.

*Corresponding author: levin@jfi.uchicago.edu

¹R. Daou, J. Chang, D. LeBoeuf, O. Cyr-Choiniere, F. Laliberte, N. Doiron-Leyraud, B. J. Ramshaw, R. Liang, D. A. Bonn, W. Hardy *et al.*, *Nature (London)* **463**, 519 (2010).

²V. Hinkov, P. Bourges, S. Pailhes, Y. Sidis, A. Ivanov, C. D. Frost, T. G. Perring, C. T. Lin, D. P. Chen, and B. Keimer, *Nature Phys.* **3**, 780 (2007).

³J. Corson, R. Mallozzi, J. Orenstein, J. N. Eckstein, and I. Bozovic, *Nature (London)* **398**, 221 (1999).

⁴L. Li, Y. Wang, S. Komiya, S. Ono, Y. Ando, G. D. Gu, and N. P. Ong, *Phys. Rev. B* **81**, 054510 (2010).

⁵L. S. Bilbro, R. V. Guilar, B. Logvenov, O. Pelleg, I. Bozovic, and N. P. Armitage, *Nature Phys.* **7**, 298 (2011).

⁶L. S. Bilbro, R. ValdesAguilar, G. Logvenov, I. Bozovic, and N. P. Armitage, *Phys. Rev. B* **84**, 100511(R) (2011).

⁷Q. J. Chen, J. Stajic, S. Tan, and K. Levin, *Phys. Rep.* **412**, 1 (2005).

⁸Q. J. Chen, I. Kosztin, B. Jankó, and K. Levin, *Phys. Rev. Lett.* **81**, 4708 (1998).

⁹D. Wulin, B. M. Fregoso, H. Guo, C.-C. Chien, and K. Levin, *Phys. Rev. B* **84**, 140509(R) (2011).

¹⁰H. Guo, D. Wulin, C.-C. Chien, and K. Levin, *New J. Phys.* **13**, 075011 (2011).

¹¹H. Guo, D. Wulin, C.-C. Chien, and K. Levin, *Phys. Rev. Lett.* **107**, 020403 (2011).

¹²H. Guo, C.-C. Chien, and K. Levin, *Phys. Rev. Lett.* **105**, 120401 (2010).

¹³Q. Chen and K. Levin, *Phys. Rev. B* **78**, 020513(R) (2008).

¹⁴A. Levchenko, T. Micklitz, M. R. Norman, and I. Paul, *Phys. Rev. B* **82**, 060502(R) (2010).

¹⁵J. Maly, B. Jankó, and K. Levin, *Physica C* **321**, 113 (1999).

¹⁶J. Maly, B. Jankó, and K. Levin, *Phys. Rev. B* **59**, 1354 (1999).

¹⁷Q. Chen, Ph.D. thesis, University of Chicago, 2000.

¹⁸C.-C. Chien, Y. He, Q. Chen, and K. Levin, *Phys. Rev. B* **79**, 214527 (2009).

¹⁹I. Kosztin, Q. J. Chen, Y.-J. Kao, and K. Levin, *Phys. Rev. B* **61**, 11662 (2000).

²⁰J. T. Stewart, J. P. Gaebler, and D. S. Jin, *Nature (London)* **454**, 744 (2008).

²¹D. Wulin, H. Guo, C.-C. Chien, and K. Levin, *Phys. Rev. B* **86**, 134518 (2012).

²²Y. S. Lee, K. Segawa, Z. Q. Li, W. J. Padilla, M. Dumm, S. V. Dordevic, C. C. Homes, Y. Ando, and D. N. Basov, *Phys. Rev. B* **72**, 054529 (2005).

²³W. S. Lee, I. M. Vishik, K. Tanaka, D. H. Lu, T. Sasagawa, N. Nagaosa, T. P. Devereaux, Z. Hussain, and Z. X. Shen, *Nature (London)* **450**, 81 (2007).

²⁴Q. J. Chen, J. Stajic, S. N. Tan, and K. Levin, *Phys. Rep.* **412**, 1 (2005).

²⁵V. M. Loktev, R. M. Quick, and S. G. Sharapov, *Phys. Rep.* **349**, 1 (2001); V. M. Loktev and S. G. Sharapov, *Low Temp. Phys.* **23**, 132 (1997); V. M. Loktev, Y. G. Pogorelov, and V. M. Turkowski, *Int. J. Mod. Phys. B* **17**, 3607 (2003); V. M. Loktev and V. M. Turkowski, *Low Temp. Phys.* **32**, 802 (2006).

²⁶C. C. Chien, Q. J. Chen, and K. Levin, *Phys. Rev. A* **78**, 043612 (2008).